• **Title**

Expression of insect α6-like nicotinic acetylcholine receptors in *Drosophila melanogaster* highlights a high level of conservation of the receptor:spinosyn interaction

• **Author names and affiliations.**

Trent Perry[1] – corresponding author.
Jason Somers[1]
Ying Ting Yang[1]
Philip Batterham[1]

[1]Bio21 Institute - Genetics Department, The University of Melbourne, Parkville, 3010, Victoria, Australia

trentp@unimelb.edu.au

j.somers@pgrad.unimelb.edu.au

ytyang@unimelb.edu.au

p.batterham@unimelb.edu.au

• **Corresponding author.**

Trent Perry

22 Bio21 Institute – Genetics Department, The University of Melbourne, 30
23 Flemington Road Parkville, Victoria Australia 3010.
24 Phone: +61383442362
25 Fax: +61393475352
26 Email: trentp@unimelb.edu.au
27

Abstract

Insecticide research has often relied on model species for elucidating the resistance mechanisms present in the targeted pests. The accuracy and applicability of extrapolations of these laboratory findings to field conditions varies but, for target site resistance, conserved mechanisms are generally the rule rather than the exception (Perry et al., 2011). The spinosyn class of insecticides appear to fit this paradigm and are a pest control option with many uses in both crop and animal protection. Resistance to spinosyns has been identified in both laboratory-selected and field-collected pest insects.

Studies using the model insect, *Drosophila melanogaster*, have identified the nicotinic acetylcholine receptor subunit, *Dα6* as an important target of the insecticide spinosad. (Perry et al., 2007; Watson et al., 2010). Field-isolated resistant strains of several agricultural pest insects provide evidence that resistance cases are often associated with mutations in orthologues to *Dα6* (Baxter et al., 2010; Puinean et al., 2013).

The expression of these receptors is difficult in heterologous systems. In order to examine the biology of the Dα6 receptor subunit further, we used Drosophila as a model and developed an *in vivo* rescue system. This allowed us to express four different isoforms of Dα6 and show that each is able to rescue the response to spinosad. Regulatory sequences upstream of the *Dα6* gene able to rescue the resistance phenotype were identified. Expression of other *D. melanogaster* subunits revealed that the rescue phenotype appears to be *Dα6* specific. We also demonstrate that expression of pest insect orthologues of Dα6 from a variety of species are capable of rescuing the

spinosad response phenotype, verifying the relevance of this receptor to resistance monitoring in the field. In the absence of a robust heterologous expression system, this study presents an *in vivo* model that will be useful in analysing many other aspects of these receptors and their biology.

Keywords

Spinosyn

Spinosad

Nicotinic acetylcholine receptor

Insecticide resistance

Drosophila melanogaster

Pest insect

[1]Abbreviations

[1] nAChR – nicotinic acetylcholine receptor

1. Introduction

1.1 The targets of insecticides are often conserved, as are target-site mediated resistance mechanisms.

Many insecticides target receptors that mediate neurotransmission. Disruption of this crucial and sensitive system leads to the rapid death of pest insects with low chemical concentrations - highly desirable commercial properties for an insecticide. However, the nervous system of insects has proven to have an inbuilt plasticity, whereby evolution can select for resistance via the modification, or even loss, of a neural receptor, overcoming this severe selection pressure (Perry et al., 2011). This should not be surprising as many insecticides emulate naturally produced plant defence compounds (e.g. pyrethrin and nicotine) to which insects have likely been exposed throughout their evolutionary histories.

In some cases the precise target and mode of action of insecticides has been discovered using the model insect, *Drosophila melanogaster* (Perry et al., 2011). That targets identified in *D. melanogaster* have typically been shown to be the targets in pests (Perry et al., 2011), underscores the evolutionary conservation of receptors involved in insect neurotransmission. Therefore the extensive genetic/genomic resources and technologies available in *D. melanogaster* can be used to identify pest insect targets, even before resistance evolves in the field (McKenzie and Batterham, 1998).

Beyond being useful for pest control, neurotoxic insecticides are agonists, antagonists, non-competitive blockers or allosteric modulators that can be powerful reagents in examining the biology of different receptor classes, particularly when used in *D. melanogaster*. An example of this is

provided by the GABA-gated chloride channel subunit encoded by *Rdl*, targeted by dieldrin (Ffrench-Constant, 1994) which depending on its co-assembled subunits has varying sensitivities to picrotoxin and bicuculline (Zhang et al., 1995) and was probed for its role in sleep using the drug, carbamazepine, also using the resistant allele, Rdl^{A302S} (Agosto et al., 2008).

1.2 The Spinosyn class of insecticides target nAChR subtypes that contain α6-like subunits and mutations in these can confer resistance

Spinosad is a mixture (85:15) of two compounds, spinosyns A and D respectively, first identified as a fermentation product from a soil actinomycete, *Saccharopolyspora spinosa* (Kirst, 2010). The characterization of Dα6 as a spinosad target in *D. melanogaster* (Perry et al., 2007; Watson et al., 2010), has been followed by reports that in Diamondback Moth, (*Plutella xylostella*), mutations causing truncations of the *Dα6* orthologue, *Pxα6* are associated with recessive spinosad resistance up to 18,600-fold (Baxter et al., 2010). This phenomenon has also been reported in *Bactrocera dorsalis* (Oriental fruit fly) conferring 901-fold resistance (Hsu et al., 2012). Recently a single point mutation (G275E) in the *Frankliniella occidentalis* (Western flower thrip) orthologue, *Foα6*, was reported to be associated with >350,000-fold spinosad resistance in a laboratory-selected strain and detected in a field collected population (Puinean et al., 2013). It has also been associated with field resistance to spinosad in the melon thrip, *Thrips palmi* (Bao et al., 2014).

While there are examples of spinosad resistance that may be explained by other mechanisms (Gao et al., 2007; Herron et al., 2014; Hojland et al., 2014; Hou et al., 2014), the commonality of this mechanism where a

117 significant loss of function of a neural receptor subunit leads to survival of the
118 insect, even at high insecticide concentrations, highlights the need to better
119 understand the biology of insect nAChRs, particularly the Dα6 subunit and its
120 orthologues. The insect *α6* gene is highly conserved. Alternative splicing and
121 RNA editing of transcripts of this gene are likely to produce α6 subunits
122 varying in pharmacological and/or electrophysiological responses when
123 assembled into pentameric receptor complexes (Grauso et al., 2002).
124
125 **1.3 Current technical limitations on studying the α6-like receptors**
126 A number of technical difficulties currently prevent robust expression of
127 many insect nAChRs *in vitro*, hampering functional studies. Heterologous
128 expression requires co-expression of a vertebrate structural β subunit for
129 many nAChR subunits, but this method was unsuccessful for Dα6 subunits
130 (Lansdell and Millar, 2004). Dα5, Dα6 and Dα7 have highest similarity to the
131 vertebrate α7 receptor which is capable of forming functional homo- and
132 hetero-pentameric receptor complexes. In oocyte expression studies Dα6 co-
133 expression with Dα5 and the accessory protein RIC3 yielded an
134 electrophysiological response to Acetylcholine (ACh) and spinosynA (Watson
135 et al., 2010), while a more recent study showed that Dα6 can assemble into
136 ACh responsive receptors with Dα5 or Dα5 and Dα7, as long as the RIC3
137 protein is co-expressed (Lansdell et al., 2012). The spinosyn sensitivity of the
138 Dα5/Dα6/Dα7 heteromeric nAChR has thus far not been reported. To
139 overcome difficulties studying the receptor *in vitro*, we have developed an *in*

vivo rescue system to characterize several aspects of insect α6 subunit biology and the response to spinosyns.

1.4 Creation of an *in vivo* system for characterising α6 receptor biology

We have used chemical mutagenesis to generate two *D. melanogaster* mutants that are highly resistant to spinosad and then successfully rescued the resistance phenotype through the expression of Dα6 isoforms, creating a powerful tool for analysing Dα6 biology. Applying the system towards studying regulation of these receptors we have identified a region upstream of *Dα6* that is capable of rescuing the susceptible phenotype when used to drive the expression of a wildtype subunit. Using this system to analyse pest insects, we have expressed *Dα6* orthologues from three species and show that each has some capacity to restore a response to spinosad.

2. Material and methods

2.1 Fly strains

Table 1. *Drosophila melanogaster* lines used in this study

Name	Origin	Genotype	Stock #
Armenia[14]	DGRC[1]	Isofemale line from Armenia[60]	103394
elavc155	BDSC[2]	P{w$^{+mW.hs}$=GawB}elav[C155]	458
Df556	BDSC[2]	w*; Df(2L)s1402, P{w^{+mC}=lacW}s1402/CyO	556
ΦX-86Fb	Basler Lab	y w M{eGFP.vas-int.Dm}ZH-2A;+;M{RFP.attP}ZH-86Fb;+	(Bischof et al., 2007)
Dbal	Batterham lab stock	*w;If/CyO;MKRS/TM6b,Tb*	
w^{1118}	BDSC[2]	*w^{1118}*	5905
4775	BDSC[2]	w^{1118}; P{w[+mC]=UAS-GFP.nls}14	4775

[1.] Drosophila Genetic Resource Centre

[2.] Bloomington Drosophila Stock Centre

Table 2. *Drosophila melanogaster* lines generated in this study

Name	Genotype	Method	Use
dα6^{W337*}	*dα6^{W337*}*	EMS mutagenesis	Spinosad resistant
dα6^{nx}	No *dα6* expression	EMS mutagenesis	Spinosad resistant

FKBP59>GAL4	w^{1118};+;pPTGAL4-{ FKBP59_0.6kb}	P-element transgenic	Enhancer analysis
Dα6>GAL4	w^{1118}, pC3G4-{ Dα6_1.1kb};+;+	P-element transgenic	Enhancer analysis

2.2 Media preparation

Standard fly media (Perry et al., 2012) was used for both rearing and bioassays of the flies. Larvae for bioassays were collected using laying plate media (Perry et al., 2012).

2.3 Bioassays

Resistance was assayed using general media dosed with appropriate concentrations of Success™ (Dow Agrosciences, 1g/L spinosad) prior to setting as per previous studies (Perry et al., 2012). Vials, each containing 50 1st instar larvae, were kept in the dark at 25°C until adult eclosion was recorded at 16-18 days.

2.4 Creation of Dα6 alleles resistant to spinosad

The *Dα6* recessive alleles used in this study (*dα6*^{W337*}, *dα6*^{nx}; Table 2) were generated using ethyl methanesulfonate (EMS) mutagenesis (Smyth et al., 1992). Approximately 250,000 embryos produced by 3000 mutagenised Armenia[14] males crossed to 5000 Df556 (spinosad resistant (Perry et al., 2007)) virgin females screened with a dose of 5ppm spinosad (Success™). These were balanced using Dbal, made homozygous and the *dα6*^{W337*} transcript was cloned using RT-PCR on isolated RNA and then sequenced.

The *Dα6* exons were also amplified from genomic DNA and sequenced for any changes in the *dα6*^{W337*} and *dα6*^{nx} alleles. The sequence reads of the transcript with the W337* change in *dα6*^{W337*} are shown (Supplementary figure 1).

2.5 Generating transgenic UAS expression constructs

Table 3. Alternate splicing and A-to-I RNA editing status of UAS-α6 constructs used in this study.

Construct	Alternate exons	A-to-I RNA edited sites [1]
UAS-Dα6-3a8a [2]	3a, 8a	4, 5 & 6
UAS-Dα6-3b8b	3b, 8b	4, 5 & 6
UAS-Dα6-3b8a	3b, 8a	4, 5, 6 & 7
UAS-Dα6-3a8b [2]	3a, 8b	4, 5 & 6
UAS-Mdα6-3b8a	3b, 8a	4, 5, 6 & 7
UAS-Bovα6-3a8b [3]	3a, 8b	4 & 6 Site 7 - K
UAS-Bovα6-3a8a [4]	3a, 8a	Site 7 - K
UAS-Pxα6-3a8b	3a, 8b	5 & 6 Site 7 - K

[1.] RNA editing sites numbered according to (Grauso et al., 2002). [2.] Constructs created artificially using an EcoRV cut site. [3.] KP231338 and [4.] KP231337. - Genbank Accession numbers.

194

195 **2.5.1 Cloning of Drosophila *Dα6* isoforms, Dα1, Dα5 and Dα7.**

196 cDNA made using RNA isolated from homozygous Armenia[14] flies was
197 PCR amplified (with respective subunit gene primers - Table 4). The products
198 were cloned using standard methods into the pGEM-T-easy vector (Promega)
199 and sequenced (Macrogen - Korea). Selected Dα6, Dα1, Dα5 and Dα7
200 clones were digested with NotI or EcoRI and ligated into respectively digested
201 pUASattB (Bischof et al., 2007). Dα6-3a8a and Dα6-3a8b isoforms were
202 artificially reconstructed from cDNA clones using a NotI/EcoRV double digest.
203 Bands of the correct size were gel purified and the appropriate ones ligated
204 into the pUASattB vector. Correctly oriented clones were then sequenced
205 (Table 3).

206

207 **2.5.2 Microinjection of *α6* UAS constructs**

208 Transgenic Drosophila were produced using a standard procedure for
209 embryonic injections into ΦX-86Fb. Plasmid DNA (Qiagen Midiprep Kit, 100-
210 250ng/ul) was injected into the posterior pole of dechorionated 0-30 minute
211 old embryos under paraffin oil using a Femtojet with a FemtoII needle
212 (Eppendorf). For ORFs of the non-drosophilid insect *α6* orthologues, ΦX;
213 $d\alpha6^{W337*}$;86Fb and ΦX; $d\alpha6^{nx}$;86Fb lines were generated and homozygous
214 lines were established from correctly mapped insertions.

215

216 **2.6 Microinjection into the w^{1118} line**

217 **2.6.1 Analysis of the *Dα6* enhancer region**

To create the *Dα6* enhancer element strains, Δ2-3 transposase plasmid DNA (100ng/ul) was co-injected with a plasmid midiprep (Qiagen) of the construct (300ng/ul) into w^{1118}. pPTGAL (DGRC 1225) was used for FKBP59>GAL4 and pC3Gal4 (DGRC 1224) was used for Dα6>GAL4. These insertions were mapped to chromosomes using Dbal, made homozygous and then crossed into the $dα6^{nx}$ and $dα6^{W337*}$ backgrounds.

2.7 Table 4. Primers used in this study.

Primer	Sequence 5'->3'	Use
Da6_enhL	CGCTAATTTTCCCACTCTGC	Dα6 enhancer
Da6_enhR	CGCATATGTTTCAAAATGACG	Dα6 enhancer
Da6_12F	AAYTGYATHATGTTYATGGT	Degenerate PCR
Da6_14R	CATNGCNGCRAAYTTCCAYTC	Degenerate PCR
Da6_cloneR	GCTTCCGACGTATCCGTAGC	Expression construct
Da6_cloneF	GTAGCCATTCAACCCGAGAG	Expression construct
Bova6_cloneF	CGGACAATTCTGGAGGGA	Expression construct
Bova6_cloneR	CAGAGAGCACCTCCATGAC	Expression construct
Ma6F	CGCACCAACCAACCAACTCAGC	Expression construct
Ma6R	AGGTTTCTTGCATTGTTGTTGTTGTCTCA	Expression construct
Bova6RACE_F	TGTGTTTCTGCTATGGCTGCCTTG	RACE

Bova6RACE_R	CACTTCTGCTTCTTCGTCGGCTTT	RACE
Da6_RT_L1	CAATATCTGGCTCCCAAACC	Real Time PCR
Da6_RT_R1	TCGTGAAGAGCGTGAAAACAA	Real Time PCR
CG13220_RTF	TGGGCAGTGCCTTCTACATTT	Real Time PCR
CG13220_RTR	CGTACGCACCTCGCTTGTT	Real Time PCR
Da1cloneF	GTTGGACCTGGCCTAAGATG	Expression construct
Da1cloneR1	CGCAATGTTCACTTCACTTCG	Expression construct
Da7cloneF	GATATAGAATATTCGAACTC	Expression construct
Da7cloneR	CAGCATCGCTCCTTCGCTTACG	Expression construct
Da5cloneF	GTAGAGAGCAGACAACATATCC	Expression construct
Da5cloneR	CCATATGGCTACGAGACAATA	Expression construct

2.8 Pest insect expression constructs

2.8.1 Cloning of *Bovα6*

Subunits from *Bovicola ovis* were cloned using a combination of degenerate primers and 5' and 3' RACE. Samples of *B. ovis* were collected from sheep based at Yeerongpilly, QLD Australia (Queensland DPI) in 2006. These samples were stored in RNAlater™ (Life Technologies) and processed using TRIzol™ (Life Technologies) as per the manufacturers protocol. The Da6_12F/Da6_14R degenerate primers were used to amplify some of the *Boα6* coding region using PCR and an amplified product was sequenced (Australian Genome Research Facility - AGRF). This allowed the design of

the *B. ovis* specific Bova6RACE_F and Bova6RACE_R primers (section 2.7). The 3' and 5' RACE (SMART™ RACE cDNA Amplification Kit, Clontech) reaction products were sequenced (AGRF) to identify start and terminal sequences and primers designed to clone the full length open reading frame (Bova6_cloneF/ Bova6_cloneR). This ORF was then sub-cloned into pUASattB (Table 3), sequenced again and transgenic lines established as per section 2.5.2.

2.8.2 *Mdα6 construct*

The *Mdα6* gene sequence had been previously published (Gao et al., 2007) and the primer sequences from that study (Ma6F/Ma6R) were used to clone the coding region out of cDNA made from RNA from a *Musca domestica* spinosad susceptible strain, WHO/I (Novartis Animal Health, Basel, Switzerland). This was cloned into pUASattB (Table 3), sequenced and transgenic lines were established as per section 2.5.2.

2.8.3 *Pxα6 construct*

A clone of the *Plutella xylostella* α6-like subunit ORF (S.W. Baxter) and this was sub-cloned into pUASattB (Table 3). Transgenic *D. melanogaster* lines were established as per section 2.5.2.

2.9 Driving the UAS constructs in the resistant backgrounds

2.9.1 Creation of elav>GAL4

The X-linked elavc155 driver was crossed separately into the background of $d\alpha6^{W337*}$ or $d\alpha6^{nx}$ (chromosome 2) to create what will be referred to as elav>GAL4 driver lines, homozygous for the driver and the

respective resistant allele. These lines were tested for resistance by screening on media containing spinosad and also for a maintained neural expression pattern, visualized by crossing to line 4775 (UAS:nGFP). These lines were then used as females in any crosses to UAS-α6 expression constructs.

2.9.2 The enhancer region of *Dα6*

For analysis of the *Dα6* upstream region, primers were designed to amplify a 1.692kb distal intergenic region (2L:9886130..9887821, Flybase release 6.02) from just inside the *Dα6* transcript start to 184bp prior to the FKBP59 transcription start site. This 1.692kb region was sub-divided into 623bp and 1069bp fragments using an EcoRI restriction site (2L:9887199), (Figure 1A). These two smaller fragments were cloned into either PC3G4 or PPTGAL4 and transgenic lines Dα6>GAL4 and FKBP59>GAL4 created (section 2.6.1).

2.10 Real Time Quantitative RT-PCR

80-100 first-instar larvae were collected and snap frozen for each sample. Total RNA was isolated using TRIzol™ reagent (Life Technologies). Each RNA sample was treated with RNase-free DNase I (Promega). 1 ug of RNA sample was used in each reverse transcription reaction using Superscript™ III Reverse Transcriptase (Life Technologies) and oligo$(dT)_{20}$. To use the $2^{-\Delta\Delta CT}$ method, each set of primers was validated against the control gene primer (Livak and Schmittgen, 2001). Real Time quantitative PCR was carried out using a QuantiFast™ SYBR green PCR kit (Qiagen) and performed on the RotorGene™-3000 (Corbett). PCR conditions were 95°C for

15 mins, followed by 50 cycles of 95°C for 30 sec, 61°C for 30 sec and 72°C for 30sec. Analysis was done using the $2^{-\Delta\Delta CT}$ method (Livak and Schmittgen, 2001). MIQE Table is presented as Supplementary Table 1.

3. Results and Discussion.

3.1 Generation of spinosad resistant alleles

Two highly resistant *Dα6* mutants were isolated from an EMS mutagenesis and selection experiment, *dα6^{W337*}* and *dα6^{nx}* (Section 2.4). These alleles confer recessive resistance to spinosad (Somers et al., 2015) and are allelic as determined by complementation testing (not shown). Mutants homozygous for *dα6^{W337*}* are 61-fold resistant compared to the parental Armenia[14] while *dα6^{nx}* are over 1000-fold more resistant (Table 5). PCR and sequencing of cDNA isolated from *dα6^{W337*}* adult RNA revealed a nucleotide G->A transition in exon 9 that changes the W^{337} codon to a termination codon. Sequencing of genomic DNA from the coding exons of *Dα6* confirmed this nucleotide change in exon 9, an exon common to all alternative splice isoforms.

Table 5. Resistance values of spinosad resistant alleles in this study

	Armenia^{14} (1)	***dα6^{W337*}***	***dα6^{nx}***
LC_{50} (95%CI)	0.034ppm (0.029-0.039)	2.09ppm (1.74-2.51)	>40ppm
Resistance ratio	1	61-fold	>1176-fold

[1] Somers et al., 2015.

No transcript was detected for *dα6^{nx}* using PCR (Da6cloneF / Da6cloneR) on cDNA generated from RNA isolated from this line (not shown). This lack of *Dα6* expression was supported by Real Time PCR (primers Da6_RT_L1/Da6_RT_R1) which did not detect expression of *Dα6* transcripts in the *dα6^{nx}* background control cross elav>GAL4xΦX-86Fb (Supplementary Figure 2). Sequencing of all exons from genomic DNA did not reveal any non-synonymous changes in the coding region of *dα6^{nx}*. While the causal molecular lesion is unknown for *dα6^{nx}*, the evidence suggests it is an allele of *Dα6* that lacks expression of wildtype *Dα6* transcripts.

The resistance level observed for the *dα6^{nx}* allele is higher than *dα6^{W337*}* suggesting that there could be some retained level of function of the Dα6 proteins produced by the truncation allele. This could be due to partially functional truncated subunits assembling into receptors and binding spinosad, or some translational read-through beyond the stop codon. For other nAChR family members there is evidence that a subunit truncated at the 4th TM domain is capable of being trafficked to the surface (Schulz et al., 2000).

The stop codon introduced by the G->A transition is 13 residues after the end of the predicted third transmembrane domain (TM3). Thus a theoretical protein would include TM3 which is implicated in spinosyn binding (Puinean et al., 2013). This mutation is at a similar position to the one found in a *P. xylostella* resistant strain (Baxter et al., 2010). In *Pxα6* a splice junction read-through leads to a frame-shift causing nonsense amino acids and a premature stop codon. It is interesting to note the resistance difference between *D. melanogaster* (61-fold) and *P. xylostella* where resistance was

initially 1080 fold with further selection on *P. xylostella* increasing this to 18,600-fold resistance. The significance of this is not clear, because while comparisons between resistant and susceptible *D. melanogaster* were undertaken in controlled genetic backgrounds, in *P. xylostella* they were not. However taken together with the over 1180-fold resistance found for a *D. melanogaster* strain with a deletion/inversion at the *Dα6* locus (Perry et al., 2007), the 370-fold adult resistance of an EMS generated *D. melanogaster* line, DAS1, an exon1/intron1 altered splice site allele (Watson et al., 2010) and the >1000-fold resistance in the $d\alpha6^{nx}$ allele, there is likely to be some retained function in the $d\alpha6^{W337*}$ truncated receptor that allows spinosad to bind and elicit a response, albeit a reduced one.

3.2 GAL4>UAS expression of individual isoforms is capable of rescuing the spinosad response phenotype of the $d\alpha6^{nx}$ and $d\alpha6^{W337*}$ alleles.

Four full length *Dα6* cDNAs including alternative exon 3 and exon 8 combinations were cloned into pUASattB (Table 3) and then inserted into the 3rd chromosome at the AttP landing site located at cytological position 86Fb (section 2.5.1 and 2.5.2). The 2nd chromosomes were replaced with one that had either the $d\alpha6^{W337*}$ allele or the $d\alpha6^{nx}$ allele, placing the rescue constructs in the resistant backgrounds. The elav>GAL4 driver was created by crossing the driver element on the X chromosome into the resistant allele background (on the 2nd chromosome) and this was used to drive expression (section 2.9.1). Each cloned isoform was crossed to the driver and bioassays performed to measure the response to spinosad, in both the $d\alpha6^{W337*}$ and

356 *dα6^{nx}* backgrounds. The data obtained measuring survival to eclosion on
357 various doses of spinosad (section 2.3) are presented in Figure 2.
358 At all spinosad doses tested for mortality (0.05ppm, 0.1ppm and
359 0.3ppm) we found that in both the *dα6^{nx}* and *dα6^{W337*}* backgrounds there was
360 a very significant level of corrected mortality (Abbott's correction (Rosenheim
361 and Hoy, 1989)) relative to the undosed media for our crosses driving
362 expression of any of the 4 isoforms of *Dα6* (Figure 2. B and D). As expected
363 the elav>GAL4 x ΦX-86Fb, expressing GAL4 (the empty AttP site), did not
364 exhibit significant mortality at any of the doses of spinosad for either
365 background (Figure 2. A and C). The insertion site, 86Fb has been reported to
366 have a level of leaky expression (Bischof et al., 2013) which we observed in
367 our insertion parentals. At a higher dose of spinosad tested (0.3ppm),
368 mortality is significantly different to that of their controls as opposed to other
369 background lines (Supplementary Tables 2 and 3). Interestingly there is a
370 significant difference in mortality for the different isoforms expressed in the
371 same genetic background. This suggests that some isoforms are more
372 responsive to spinosad or better able to form functional receptors than others.
373 This could possibly be due to sequence differences between isoforms
374 impacting the binding site or receptor responsiveness.
375 *dα6^{nx}* and *dα6^{W337*}* rescue experiments show that each of the
376 individual isoforms is capable of rescuing the response to spinosad. There is
377 no observed difference in the mortality of the background strains or insertion
378 parentals to undosed media or 0.05ppm spinosad for either resistant
379 background (Figure 2). This shows that both alleles are suitable for analyzing
380 rescue. While in both resistant backgrounds the parental isoform strains show

a level of mortality, quite clearly at the 0.3ppm dose (Supplementary Tables 2 and 3) this is easily distinguishable from the observed mortality for the elav>GAL4 driven isoforms.

3.3 Analysis of the *Dα6* enhancer region

3.3.1 The region upstream of *Dα6* contains enhancer elements

A 1.692kb intergenic region between the *FKBP59* and *Dα6* genes was cloned and it was also sub-cloned into 1.1kb and 0.6kb fragments to analyse the expression driven by this region (Figure 1A and Section 2.9.2). Initially the vector pStinger was used to examine the expression pattern, this placed nGFP under the direct regulatory control of each fragment. Third instar larval brains from at least two independent insertion lines for each region were examined for nGFP expression which was present (Supplementary Figure 3). The same elements were then cloned into GAL4 expression vectors (Section 2.9.2). These constructs were crossed to line 4775 to drive nGFP, allowing visualisation of the expression. The expression patterns observed of the pStinger and the PC3G4/pPTGAL4 constructs in 3rd instar larval brains were extremely similar (Supplementary Figure 3). We examined the expression of the two enhancers using a pStinger FKBP59_0.6kb line (GFP) and a UAS:RFP insertion driven by the Dα6>GAL4 line. This cross showed the expression patterns of GFP and RFP to be non-overlapping (Figure 1C).

3.3.2 Expression pattern of Dα6>GAL4.

The Dα6>GAL4 driver appears to express nGFP in the cortex of the central brain, most likely in nuclei of cell bodies with projections into the

406 mushroom bodies (Figure 1B and C.). There is additional nGFP possibly in
407 the cortex of the ventral ganglion. The 1.1kb fragment is adjacent to the *Dα6*
408 gene and it is likely that the nGFP marks at least a subset of cells that would
409 express *Dα6*.
410
411 **3.3.3 FKBP59>GAL4 expression pattern.**
412 FKBP59>GAL4 drives expression of nGFP in a non-overlapping
413 pattern to that of Dα6>GAL4 with a noticeable difference in expression in the
414 central brain (Figure 1C). It appears to be either in glial cells or in the central
415 brain cortex but in different cell bodies to those expressing nRFP driven by
416 Dα6>GAL4. There is also nGFP visualised in the ventral ganglion,
417 concentrated in the outer cell layer that would again suggest a glial cell
418 expression. It is also expressed at several other locations in larvae including
419 the salivary glands, a common expression artefact observed with the
420 pPTGAL4 vector rather than the enhancer itself (Sharma et al., 2002).
421
422 **3.3.4 The response to spinosad is dependent on the expression pattern**
423 **of *Dα6*.**
424 Driver lines were used to express the UAS-Dα6-3b8b isoform in the
425 $d\alpha6^{nx}$ background and assayed for their mortality on doses of spinosad. The
426 Dα6>GAL4 driver line was able to rescue the resistance phenotype (Figure
427 1D), however the FKBP59>GAL4 did not. This was found for a second,
428 independent FKBP59>GAL4 insertion line (not shown). The Dα6>GAL4
429 driving expression of UAS-Dα6-3b8b in the $d\alpha6^{W337*}$ background, confirmed a
430 capacity to rescue the spinosad response (Supplementary Table 4).

The corrected mortality shows a lower response to spinosad when compared to the rescue observed for the elav>GAL4 driver. At the lowest dose of 0.05ppm spinosad, in the *dα6^{nx}* background, the elav>GAL4 corrected mortality (86 +/- 4) when compared to that of the Dα6>GAL4 (41 +/- 9) indicates there is likely to be a higher level of expression when using elav>GAL4 and/or a greater number of cells expressing *Dα6* than when using Dα6>GAL4 to drive expression. This was examined using Real time RT-PCR (Supplementary Figure 2). The Quantitative Real time RT-PCR examined the levels of transcription from several drivers in crosses performed in the *dα6^{nx}* background. A low level of background expression was confirmed for the 86Fb AttP landing site as expected from the rescue results (Supplementary Tables 2 and 3) and published data regarding that landing site (Bischof et al., 2013). This expression is clearly distinguishable from the rescue crosses when using the elav>GAL4. There is not a significant difference in the expression from the Dα6>GAL4 compared to the parental Dα6-3b8b background that is not being driven, however they are much more susceptible to spinosad (41 corrected mortality vs -2 respectively at 0.05ppm, Figure 1D vs Figure 2B – Graph 3b8b). Given the significant increase in spinosad sensitivity observed with these drivers versus the insertion parental line, not just the level but also the localisation of expression is most certainly causing the difference in the phenotypes.

Expression occurring in cells that do not normally express Dα6 might not lead to the translation or correct assembly of receptors that are capable of responding to spinosad. This is supported by the FKBP59>GAL4 driver results that do not rescue the spinosad resistance phenotype despite

456 neuronal expression being detected (Figure 1C and D). This could be due to
457 the lack of co-expression of other nAChR subunits that might, along with Dα6,
458 form a spinosad target or to the absence of other cellular proteins required for
459 the correct folding, chaperoning and trafficking of the protein or for synapse
460 formation between adjacent cells (Nakayama et al., 2014). Even if functional
461 Dα6 containing receptors are being formed and localised to a synapse in
462 these cells, they are obviously not involved in a process where inappropriate
463 signalling due to spinosad exposure leads to mortality. The expression
464 patterns we observe for the FKBP59>GAL4 line, together with rescue results
465 indicate that it is not likely to represent the expression of *Dα6* or at least not
466 express the receptor subunit in regions where spinosad exerts its toxic effect
467 on Dα6-containing receptors. Based on the rescue results from the
468 Dα6>GAL4 driver crossed to UAS-Dα6-3b8b, the expression pattern
469 observed with nGFP was at least a partial representation of the native Dα6
470 expression pattern that includes cells involved in the response to spinosad.
471
472 **3.4 Expression of Dα1, Dα5 and Dα7 nAChR subunits does not rescue**
473 **the spinosad response.**
474 We investigated the possibility that expression of other nAChR
475 subunits in cells that normally express *Dα6* could give the same spinosad
476 phenotype. This was performed with the two most closely related subunits,
477 Dα5 (53/65% identity/similarity) and Dα7 (53/65% identity/similarity), as well
478 as Dα1 (12/26% identity/similarity) (Grauso et al., 2002). Expression was
479 driven with Dα6>GAL4 to allow rescue in a limited number of cells shown to
480 produce a spinosad response when Dα6 was expressed (Section 3.3.4).

While these subunit proteins are also being expressed from their native loci, we are effectively adding or enhancing expression levels in some Dα6 expressing cells.

Expression of Dα5, Dα7 or Dα1 subunits does not lead to any rescue of susceptibility to spinosad at either the 0.05ppm or 1ppm dose (Figure 3). This result provides evidence that the subunits examined, Dα1, Dα5 or Dα7 cannot replace the Dα6-mediated response to spinosad.

The lack of rescue by Dα7 concurs with the observation that oocyte expression of Dα6 in combination with Dα7 has a negligible or substantially inferior response to spinosad (Watson et al., 2010). Our Dα5 data suggest Dα6 is required to mediate the toxic effect of spinosad. This is despite Dα6 being unable to respond to spinosad or ACh without Dα5 co-expression in oocytes (Lansdell et al., 2012; Watson et al., 2010). Dα1 was not expected to rescue and was selected as a more distantly related nAChR subunit to Dα6. It is involved in a response to neonicotinoids and the alleles tested do not confer spinosad resistance (Perry et al., 2012).

The similarity of the Dα5/Dα6/Dα7 subunits, particularly around the protein region where the *Foα6* resistance associated mutation was reported (Puinean et al., 2013), suggests that, while spinosad might bind in this region, other domains in the Dα6 subunit could co-operatively bind spinosad. Structural and spatial constraints in Dα5 and Dα7 subunits may also prevent spinosad binding.

3.5 Expression of Dα6 orthologues can rescue the spinosad response.

505 α6-mediated spinosad resistance has been reported in a number of
506 pest insects. We therefore tested Dα6 orthologues from three taxonomically
507 diverse species, *M. domestica* (Diptera), *P. xylostella* (Lepidoptera) and *B.*
508 *ovis* (Phthiraptera) in the *D. melanogaster* expression system. Resistance has
509 been identified in *M. domestica* but there is no evidence it is linked to the α6-
510 orthologue (Gao et al., 2007). Resistance has not been reported for *B.ovis*,
511 while *Pxα6* has been directly associated with spinosad resistance (Baxter et
512 al., 2010). A protein sequence alignment illustrates the strong similarity of
513 these subunits (Figure 4). They have high homology but there are several
514 divergent regions, particularly beyond the TM3 domain, generally found to be
515 the least conserved region among nAChR subunits.
516 In order to have the best chance of detecting a spinosad response we
517 wanted to maximise the expression of these subunits in our system. Therefore
518 we used elav>GAL4 as it provided a higher spinosad response and more
519 mRNA (Figures 2B vs 1D, and Supplementary Figure 2). Expression in the
520 $d\alpha6^{nx}$ background with elav>GAL4, results in phenotypic rescue with each of
521 the three *Dα6* orthologues (Figure 5 A-C). The *P. xylostella* orthologue
522 confers sensitivity at 0.1ppm. Indeed the UAS-*Pxα6-3a8b* parental shows an
523 even higher spinosad response than that observed with any Drosophila
524 isoform parental line in the $d\alpha6^{nx}$ background (Figure 2B vs 5B). This is more
525 noticeable at higher doses (Supplementary Table 2 vs Figure 5B 0.3ppm
526 dose).
527 The UAS-Mdα6-3b8a *M. domestica* isoform was tested in the $d\alpha6^{nx}$
528 background and the spinosad susceptible phenotype is rescued at 0.3ppm
529 (Figure 5A). In the $d\alpha6^{W337*}$ background there is a response at 0.1ppm,

highlighting the more susceptible nature of this allele (Supplementary Table 5). This could possibly be due to interactions of the proteins with the truncated Dα6 protein.

The UAS-Pxα6-3b8a cross to elav>GAL4 provides a higher level of response to spinosad than any of the Drosophila isoforms (Figure 5B). This is particularly noticeable in the insertion parental line where there is a marked increase in the susceptibility to spinosad compared to even the most susceptible *D. melanogaster* isoform, UAS-Dα6-3a8a (Figure 2B). This could mean that UAS-Pxα6-3b8a forms receptors that are more spinosad responsive. There are several differences between it and the Drosophila protein in the C-terminal region, the likely site of interaction with spinosad (Figure 4) (Puinean et al., 2013).

B. ovis had two isoforms cloned and expressed, UAS-Bovα6-3a8b and UAS-Bovα6-3a8a. The expression using elav>GAL4 shows both rescue the response to spinosad, albeit at slightly different levels (Figure 5C). The rescue is also lower than that of the respective *D. melanogaster* native isoforms. A clone of the 3a8a isoform has not been reported for *D. melanogaster* (Flybase: http://flybase.org/reports/FBgn0032151.html, accessed 2-Oct-2014), however we were able to artificially construct one (Section 2.5.1). It was quite responsive to spinosad when overexpressed (Figure 2B). This pattern holds for the two *B. ovis* isoforms with UAS-Bovα6-3a8b less responsive to spinosad than UAS-Bovα6-3a8a. A possibility is that in wildtype *D. melanogaster* the suppression of this 3a8a isoform is due to its pharmacological properties. Only the UAS-Bovα6-3a8b isoform was tested in

554 the *dα6*^{W337*} allele background and the results from this were similar
555 (Supplementary Table 5).
556 The two *B. ovis* isoforms only differ at 8a vs 8b and in one other
557 residue in the N-terminal ligand binding region. This, along with variations in
558 the levels of rescue observed for different *D. melanogaster* splice isoforms,
559 highlights that spinosad sensitivity is significantly impacted by the variety and
560 proportions of splice isoforms that are produced. Isoform diversity and
561 abundance will vary in different cell types in one insect species and between
562 species.
563 The difference in the levels of rescue we observe between genes from
564 different species could be due to numerous, but not necessarily independent,
565 factors. The pest genes were not codon optimised for expression in *D.*
566 *melanogaster.* Therefore the differences in nucleotide coding could affect
567 translation due to codon bias or the differences in amino acid sequence
568 between the α6-orthologues. These differences could either decrease the
569 amount of receptor translated, reduce the capacity of spinosad to bind to the
570 receptor, make the receptor less responsive even if spinosad does bind or
571 alter the binding sites of accessory proteins that are required for wildtype α6
572 containing receptors to be formed. Loss of binding interactions with
573 modulatory proteins or chaperones could lead to poorer function or impaired
574 assembly of a correct channel with other Drosophila nAChR subunits (Jones
575 et al., 2010).
576 Differences in the Bovα6 and the Pxα6 protein sequence compared with
577 other dipteran orthologues are concentrated in the C-terminal region and in
578 the TM3-TM4 cytoplasmic loop. Thus there could be important differences

579 that lead to an altered capacity for spinosad binding or in the responsiveness
580 of the channel once spinosad binds and exerts its effect. While sequence
581 differences in this region of the α6 protein seem important for the spinosad
582 response, it is not possible pinpoint in the residues involved given the number
583 of residues that differ. The expression of chimeric (Somers et al., 2015) and/or
584 *in vitro* mutagenised α6 protein would be required to increase the resolution of
585 this analysis.

586 Besides the isoform variation between the tested constructs, there is a
587 103 amino acid stretch of almost perfect conservation between all species,
588 other than a T276S change in *B. ovis*, in transmembrane domains 1 to 3
589 (Figure 4). This level of conservation around the region predicted to have a
590 role in spinosad binding (Puinean et al., 2013) could explain the capacity of
591 spinosad to exert an effect on all of the insect α6-like isoforms tested. It also
592 suggests a potential for *α6*-mediated resistance to spinosad to evolve in many
593 insect species.

594 In recessive *dα6* mutant alleles, expression of individual isoforms of
595 Dα6 is sufficient to contribute to a spinosad binding site. Thus mutations that
596 only remove individual isoforms are not likely to confer high levels of
597 resistance, except in the case of a dominant negative allele (as observed in
598 Somers et al., 2015). This is supported by the types of mutations that have
599 thus far been identified as a cause of or associated with spinosad resistance
600 (Baxter et al., 2010; Puinean et al., 2013; Watson et al., 2010).

601 Spinosad resistance conferred by an *α6* mutation has already arisen in
602 *P. xylostella* (Baxter et al., 2010). If the *Pxα6* expression studies performed
603 here had been conducted before field resistance arose, then the genetic basis

604 of resistance would have been correctly predicted. Based on our expression
605 studies with the *M. domestica* and *B. ovis* α*6*-orthologues, there is a potential
606 for α*6*-mediated resistance to evolve in these species. The spinosad binding
607 and response observed in our test system is likely to occur in the pests
608 themselves. Spinosad resistance has not yet evolved in *B. ovis* which could
609 be due to the way in which the insecticide is used, with direct individual
610 application to the host (sheep), or the fact that there are a number of effective
611 alternative insecticides for treatment of *B. ovis* available. In *M. domestica*
612 resistance has evolved, but not via an α*6*-mediated mechanism as yet (Gao
613 et al., 2007). This could simply be because other resistance mechanisms
614 have evolved first. α6-mediated target site resistance could arise later or not
615 at all, depending on patterns of spinosad usage. Under these circumstances
616 molecular screening of pest populations for α*6* loss of function mutations may
617 be worthwhile. Loss or modification of α6 function may have greater fitness
618 costs in some species, with other mechanisms providing a better balance of
619 resistance and fitness to counter the prevailing levels of insecticide exposure.
620 Given that loss of α6 function confers resistance, mutations in genes involved
621 in the assembly and membrane localization of α6, or in maintaining synapses
622 (Nakayama et al., 2014) could confer resistance.
623
624 **4. Summary and conclusions**
625 This study demonstrates the capacity of individual insect α6 subunits to
626 rescue a response to spinosad with a high degree of sensitivity. The
627 development of a simple rescue paradigm allowed us to test and make some
628 comparisons between different species, and even within species (*D.*

melanogaster and B. ovis.) for different isoforms. The system also offers the opportunity to investigate other aspects of α6 receptor biology through this response to spinosad phenotype; artificial constructs may shed further light on critical spinosad binding regions given that robust heterologous expression systems are still being developed. There are many reasons why sensitivities differ between all the isoforms and species tested, but in this study all analysed rescue constructs had an easily detected response to spinosad, supporting the notion that α6 containing nAChRs are a conserved target of spinosad in a wide range of insect species.

Acknowledgements

The authors would like to thank the providers of materials that were used in this study; J. Bishof and K. Basler for providing their pUASattB vector, Bloomington Stock centre for fly lines, the Australian Drosophila Biomedical Research Support Facility for handling quarantine and importing flies, Novartis Animal Health for *M. domestica* WHO/I sample, Queensland Department of Primary Industries for *B.ovis* samples and S.W. Baxter for the *P. xylostella* clone. They would also like to acknowledge sources of funding for the project, Australian Research Council Discovery Grant (DP120100788 - PB) and an Australian Wool Innovation Research Fellowship (TP) and J.N. Peters Bequest Fellowship (TP).

References

Agosto, J., Choi, J.C., Parisky, K.M., Stilwell, G., Rosbash, M., Griffith, L.C., 2008. Modulation of GABAA receptor desensitization uncouples sleep onset and maintenance in Drosophila. Nat Neurosci 11, 354-359.

Bao, W.X., Narai, Y., Nakano, A., Kaneda, T., Murai, T., Sonoda, S., 2014. Spinosad resistance of melon thrips, Thrips palmi, is conferred by G275E mutation in alpha6 subunit of nicotinic acetylcholine receptor and cytochrome P450 detoxification. Pesticide biochemistry and physiology 112, 51-55.

Baxter, S.W., Chen, M., Dawson, A., Zhao, J.Z., Vogel, H., Shelton, A.M., Heckel, D.G., Jiggins, C.D., 2010. Mis-spliced transcripts of nicotinic acetylcholine receptor alpha6 are associated with field evolved spinosad resistance in Plutella xylostella (L.). PLoS Genet 6, e1000802.

664 Bischof, J., Bjorklund, M., Furger, E., Schertel, C., Taipale, J., Basler, K.,
665 2013. A versatile platform for creating a comprehensive UAS-ORFeome
666 library in Drosophila. Development 140, 2434-2442.
667 Bischof, J., Maeda, R.K., Hediger, M., Karch, F., Basler, K., 2007. An
668 optimized transgenesis system for Drosophila using germ-line-specific phiC31
669 integrases. Proc Natl Acad Sci U S A 104, 3312-3317.
670 Edgar, R.C., 2004. MUSCLE: multiple sequence alignment with high accuracy
671 and high throughput. Nucleic Acids Res 32, 1792-1797.
672 Ffrench-Constant, R.H., 1994. The molecular and population genetics of
673 cyclodiene insecticide resistance. Insect Biochem Mol Biol 24, 335-345.
674 Gao, J.R., Deacutis, J.M., Scott, J.G., 2007. The nicotinic acetylcholine
675 receptor subunit Mdalpha6 from Musca domestica is diversified via post-
676 transcriptional modification. Insect Mol Biol 16, 325-334.
677 Gouy, M., Guindon, S., Gascuel, O., 2010. SeaView version 4: A multiplatform
678 graphical user interface for sequence alignment and phylogenetic tree
679 building. Mol Biol Evol 27, 221-224.
680 Grauso, M., Reenan, R.A., Culetto, E., Sattelle, D.B., 2002. Novel putative
681 nicotinic acetylcholine receptor subunit genes, D alpha 5, D alpha 6 and D
682 alpha 7 in Drosophila melanogaster identify a new and highly conserved
683 target of adenosine deaminase acting on RNA-mediated A-to-I pre-mRNA
684 editing. Genetics 160, 1519-1533.
685 Herron, G.A., Gunning, R.V., Cottage, E.L., Borzatta, V., Gobbi, C., 2014.
686 Spinosad resistance, esterase isoenzymes and temporal synergism in
687 Frankliniella occidentalis (Pergande) in Australia. Pesticide biochemistry and
688 physiology 114, 32-37.

689 Hojland, D.H., Jensen, K.M., Kristensen, M., 2014. Expression of Xenobiotic
690 Metabolizing Cytochrome P450 Genes in a Spinosad-Resistant Musca
691 domestica L. Strain. PLoS One 9, e103689.
692 Hou, W., Liu, Q., Tian, L., Wu, Q., Zhang, Y., Xie, W., Wang, S., Miguel, K.S.,
693 Funderburk, J., Scott, J.G., 2014. The alpha6 nicotinic acetylcholine receptor
694 subunit of Frankliniella occidentalis is not involved in resistance to spinosad.
695 Pesticide biochemistry and physiology 111, 60-67.
696 Hsu, J.C., Feng, H.T., Wu, W.J., Geib, S.M., Mao, C.H., Vontas, J., 2012.
697 Truncated transcripts of nicotinic acetylcholine subunit gene Bdalpha6 are
698 associated with spinosad resistance in Bactrocera dorsalis. Insect Biochem
699 Mol Biol 42, 806-815.
700 Jones, A.K., Buckingham, S.D., Sattelle, D.B., 2010. Proteins interacting with
701 nicotinic acetylcholine receptors: expanding functional and therapeutic
702 horizons. Trends Pharmacol Sci 31, 455-462.
703 Kirst, H.A., 2010. The spinosyn family of insecticides: realizing the potential of
704 natural products research. J Antibiot (Tokyo) 63, 101-111.
705 Lansdell, S.J., Collins, T., Goodchild, J., Millar, N.S., 2012. The Drosophila
706 nicotinic acetylcholine receptor subunits Dalpha5 and Dalpha7 form functional
707 homomeric and heteromeric ion channels. BMC neuroscience 13, 73.
708 Lansdell, S.J., Millar, N.S., 2004. Molecular characterization of Dalpha6 and
709 Dalpha7 nicotinic acetylcholine receptor subunits from Drosophila: formation
710 of a high-affinity alpha-bungarotoxin binding site revealed by expression of
711 subunit chimeras. J Neurochem 90, 479-489.

712 Livak, K.J., Schmittgen, T.D., 2001. Analysis of relative gene expression data
713 using real-time quantitative PCR and the 2(-Delta Delta C(T)) Method.
714 Methods 25, 402-408.
715 McKenzie, J.A., Batterham, P., 1998. Predicting insecticide resistance:
716 mutagenesis, selection and response. Philos Trans R Soc Lond B Biol Sci
717 353, 1729-1734.
718 Nakayama, M., Matsushita, F., Hama, C., 2014. The Matrix Protein Hikaru
719 genki Localizes to Cholinergic Synaptic Clefts and Regulates Postsynaptic
720 Organization in the Drosophila Brain. J Neurosci 34, 13872-13877.
721 Perry, T., Batterham, P., Daborn, P.J., 2011. The biology of insecticidal
722 activity and resistance. Insect Biochem Mol Biol 41, 411-422.
723 Perry, T., Chan, J.Q., Batterham, P., Watson, G.B., Geng, C., Sparks, T.C.,
724 2012. Effects of mutations in Drosophila nicotinic acetylcholine receptor
725 subunits on sensitivity to insecticides targeting nicotinic acetylcholine
726 receptors. Pesticide biochemistry and physiology 102, 56-60.
727 Perry, T., Heckel, D.G., McKenzie, J.A., Batterham, P., 2008. Mutations in
728 Dalpha1 or Dbeta2 nicotinic acetylcholine receptor subunits can confer
729 resistance to neonicotinoids in Drosophila melanogaster. Insect Biochem Mol
730 Biol 38, 520-528.
731 Perry, T., McKenzie, J.A., Batterham, P., 2007. A Dalpha6 knockout strain of
732 Drosophila melanogaster confers a high level of resistance to spinosad. Insect
733 Biochem Mol Biol 37, 184-188.
734 Puinean, A.M., Lansdell, S.J., Collins, T., Bielza, P., Millar, N.S., 2013. A
735 nicotinic acetylcholine receptor transmembrane point mutation (G275E)

736 associated with resistance to spinosad in Frankliniella occidentalis. J
737 Neurochem 124, 590-601.
738 Rosenheim, J.A., Hoy, M.A., 1989. Confidence Intervals for the Abbott's
739 Formula Correction of Bioassay Data for Control Response. Journal of
740 Economic Entomology 82, 331-335.
741 Schulz, R., Bertrand, S., Chamaon, K., Smalla, K.H., Gundelfinger, E.D.,
742 Bertrand, D., 2000. Neuronal nicotinic acetylcholine receptors from
743 Drosophila: two different types of alpha subunits coassemble within the same
744 receptor complex. J Neurochem 74, 2537-2546.
745 Sharma, Y., Cheung, U., Larsen, E.W., Eberl, D.F., 2002. PPTGAL, a
746 convenient Gal4 P-element vector for testing expression of enhancer
747 fragments in drosophila. Genesis 34, 115-118.
748 Smyth, K.A., Parker, A.G., Yen, J.L., McKenzie, J.A., 1992. Selection of
749 dieldrin-resistant strains of Lucilia cuprina (Diptera: Calliphoridae) after ethyl
750 methanesulfonate mutagenesis of a susceptible strain. J Econ Entomol 85,
751 352-358.
752 Somers, J., Nguyen, J., Lumb, C., Batterham, P., Perry, T., 2015. In vivo
753 functional analysis of the Drosophila melanogaster nicotinic acetylcholine receptor
754 *Dα6* using the insecticide Spinosad. Insect Biochem Mol Biol
755 Watson, G.B., Chouinard, S.W., Cook, K.R., Geng, C., Gifford, J.M.,
756 Gustafson, G.D., Hasler, J.M., Larrinua, I.M., Letherer, T.J., Mitchell, J.C.,
757 Pak, W.L., Salgado, V.L., Sparks, T.C., Stilwell, G.E., 2010. A spinosyn-
758 sensitive Drosophila melanogaster nicotinic acetylcholine receptor identified
759 through chemically induced target site resistance, resistance gene

760 identification, and heterologous expression. Insect Biochem Mol Biol 40, 376-
761 384.
762 Zhang, H.G., Lee, H.J., Rocheleau, T., ffrench-Constant, R.H., Jackson, M.B.,
763 1995. Subunit composition determines picrotoxin and bicuculline sensitivity of
764 Drosophila gamma-aminobutyric acid receptors. Mol Pharmacol 48, 835-840.
765
766

Figures

Figure 1

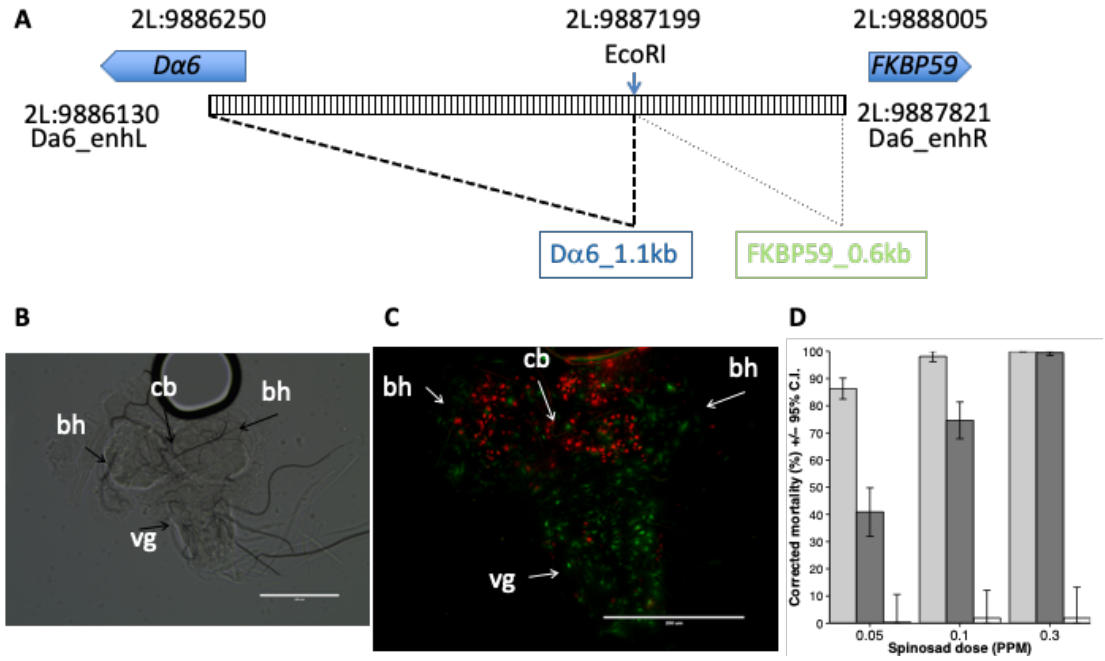

Figure 1. Analysis of the Dα6 upstream genomic region for regulatory sequences.
A. Schematic of the genome region used for creating the enhancer>GAL4 constructs. The 1.692kb region is shown as a striped box. The beginning of the surrounding genes is indicated with a solid blue arrow. Lines under the region illustrate parts of the regions that are in each GAL4 construct. The names of the driver lines created are colored according to results in D. **B.** Light image (10X) of dissected third instar larval brain viewed dorsally from C. **C.** Flattened stack composite image of RFP (1.1kb) and GFP (0.6kb) channels (20X) of dissected third instar larval brain viewed dorsally. Scale bars for B and C are 200μm. Images taken using an EVOS® FLoid® Auto (Life Technologies) Label abbreviations – bh; brain hemisphere, cb; central brain, vg; ventral ganglion. **D.** Graph of mortality results from rescue crosses with different drivers controlling expression of UAS-Dα6-3b8b in the *dα6^{nx}* background. Bars represent the UAS-Dα6-3b8b crossed with elav>GAL4 in light grey, with Dα6>GAL4 in dark grey and with FKBP59>GAL4 in white. 95% CI are shown.

Figure 2

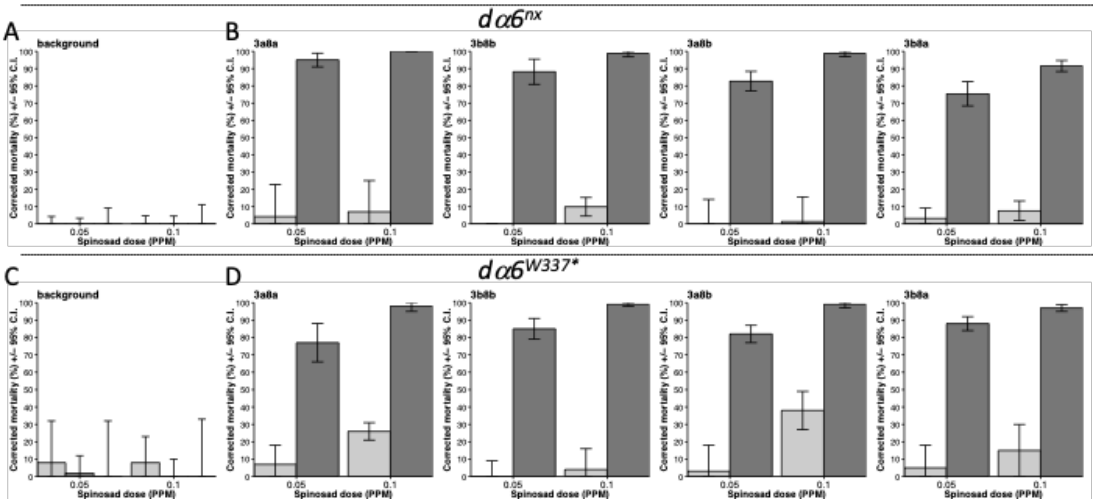

Figure 2. Rescue of the spinosad susceptible phenotype using individual isoforms of Dα6.

Mortality results are shown from rescue experiments using UAS-Dα6 isoforms in the *dα6*^{nx} and *dα6*^{W337*} backgrounds. **A and C**. Background panels show ΦX-86Fb, elav>GAL4 and elav>GAL4 x ΦX-86Fb values are not significantly different to mortality on undosed media in the *dα6*^{nx} (**A**) and *dα6*^{W337*} (**C**) backgrounds. **B and D.** The graphs are labeled with the isoform used (3a8a, 3b8b, 3a8b and 3b8a). The bars are the homozygous insertion line (light grey) and the insertion driven by elav>GAL4 (dark grey) in the *dα6*^{nx} (**B**) and *dα6*^{W337*} (**D**) backgrounds. 95% CI are shown.

Figure 3

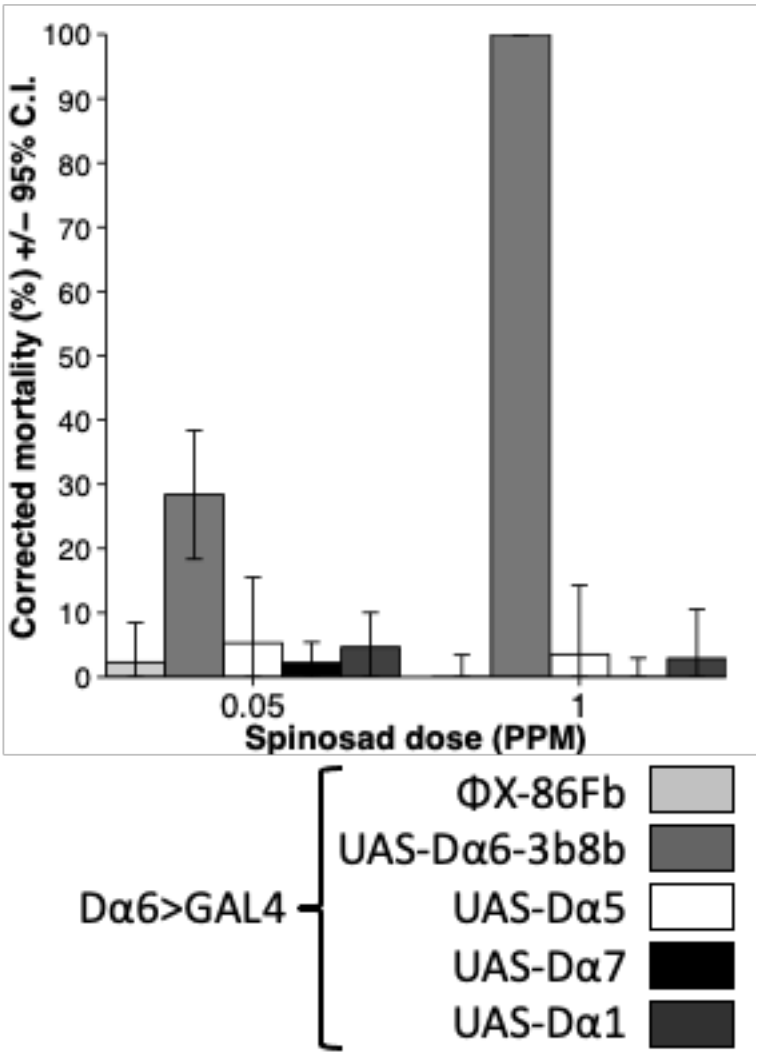

Figure 3. D*α6*>GAL4 expression of different Drosophila nAChR subunits. Mortality results are shown from ΦX-86Fb empty AttP background, UAS-Dα6-3b8b, UAS- Dα1, UAS-Dα5 and UAS-Dα7 Drosophila nAChR subunits when expressed in the *dα6*^{nx} background using Dα6>GAL4. Only the UAS-Dα6-3b8b construct was able to rescue the susceptibility to spinosad. 95% CI are shown.

Figure 4

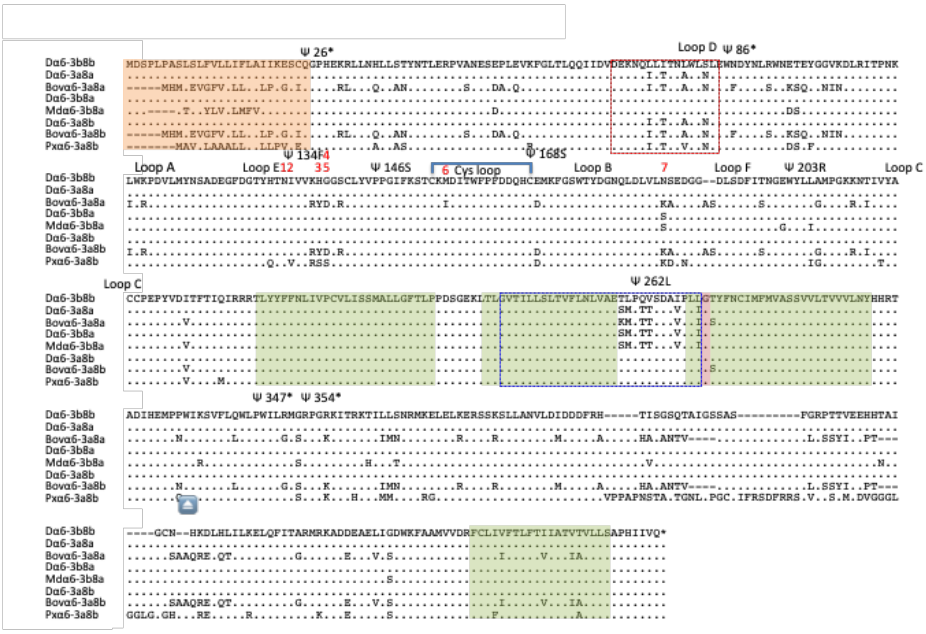

Figure 4. Protein alignment of insect α6 subunits from this study.
MUSCLE protein alignment of insect α6-like isoforms used in this study created with seaview (Gouy et al., 2010, Edgar, 2004). Predicted transmembrane domains are highlighted in green. Alternative exon 3a and 3b are in the dotted red box and alternative exon 8a and 8b in dotted blue box. Red numbering indicates RNA editing locations as per Grauso et al., 2002. The G301E mutation from *F. occidentalis*, Foα6 is boxed in red. ⏏ - site of the W337* mutation of *dα6*^{W337*} in this study and also the site of mis-splicing in a spinosad resistant strain of *P. xylostella* ((Baxter et al., 2010).

Figure 5

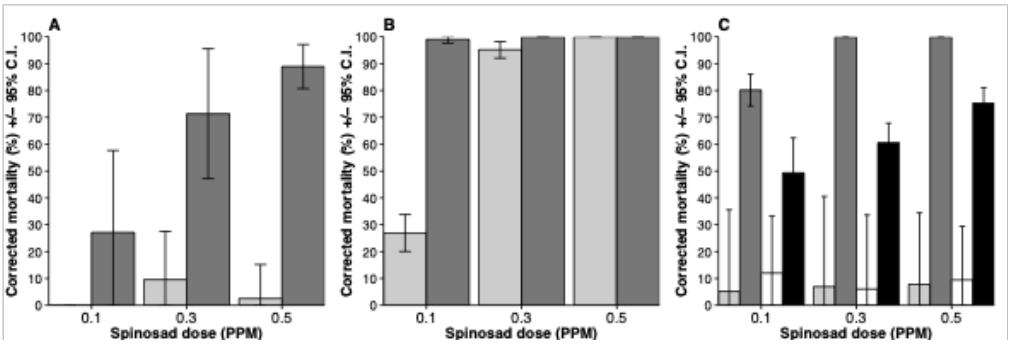

Figure 5. Pest insect α6 subunits can rescue of susceptibility on spinosad when expressed using elav>GAL4.

Mortality results when using elav>GAL4 to drive expression of UAS constructs (Table 3) in the *dα6*^{nx} background. The light shading represents the parental insertion line and dark shading represents the construct crossed to elav>GAL4. **A**. *M. domestica* rescue with the 3b8a isoform (Note the parental insertion was not tested on 0.1ppm. There was no significant difference observed in the driven construct at 0.1ppm spinosad). **B**. *P. xylostella* rescue with the 3a8b isoform. **C**. *B. ovis r*escue with the 3a8a (light grey - parental and dark grey - driven) and 3a8b (white - parental and black - driven) isoforms. 95% CI are shown.

Supplementary Figures and Tables

Figure S1. Identification of the *dα6*^{W337*} mutation

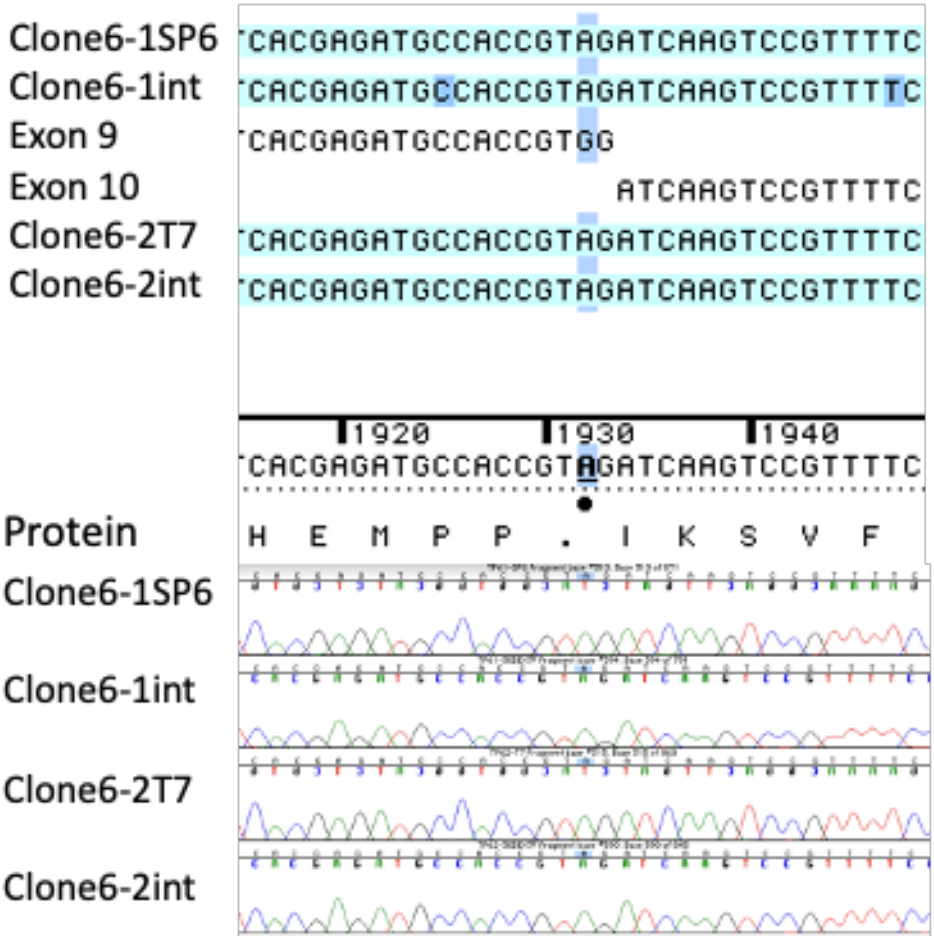

Figure S1. Identification of the *dα6*^{W337*} mutation
Sequence reads of two clones of *dα6*^{W337*} with the G>A transition causing the nonsense mutation W337* (Sequencher 4.7 Genecodes). RNA was isolated (Trizol) and cDNA made (SuperscriptIII – Invitrogen) and PCR performed on this from which products were ligated into pGEM-T-Easy and transformed. Plasmids were isolated with a miniprep kit (Promega) and sequenced at Macrogen (Korea) with vector primers T7 and SP6 and an internal primer (30DEX7F - GATTCGATGGCACGTATCAC).

Figure S2. Analysis of relative expression levels of *Dα6* transcripts

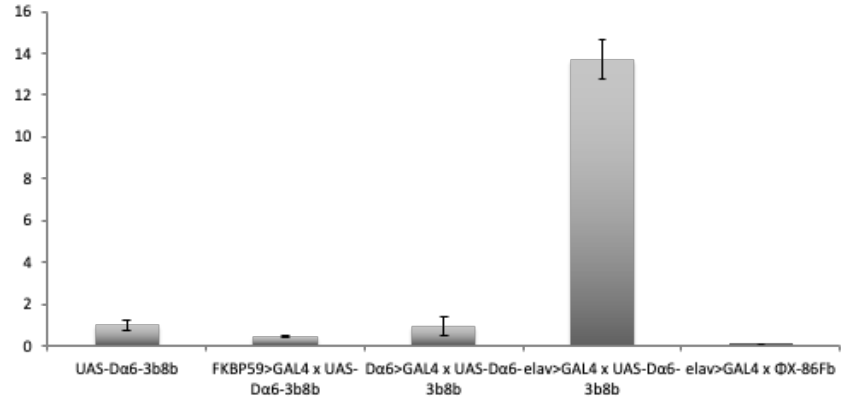

Figure S2 Analysis of relative expression levels of *Dα6* transcripts
Relative expression levels of *Dα6* transcripts in the $d\alpha6^{nx}$ background for the parental line UAS-Dα6-3b8b, (set equal to 1), and the parental line crossed to different drivers. Clearly the elav>GAL4 driver expresses the transcript at the highest level while in the $d\alpha6^{nx}$ background control cross, elav>GAL4 x ΦX-86Fb, *Dα6* transcript is barely detectable.

Figure S3. Analysis of *Dα6* enhancer constructs in pStinger vector.

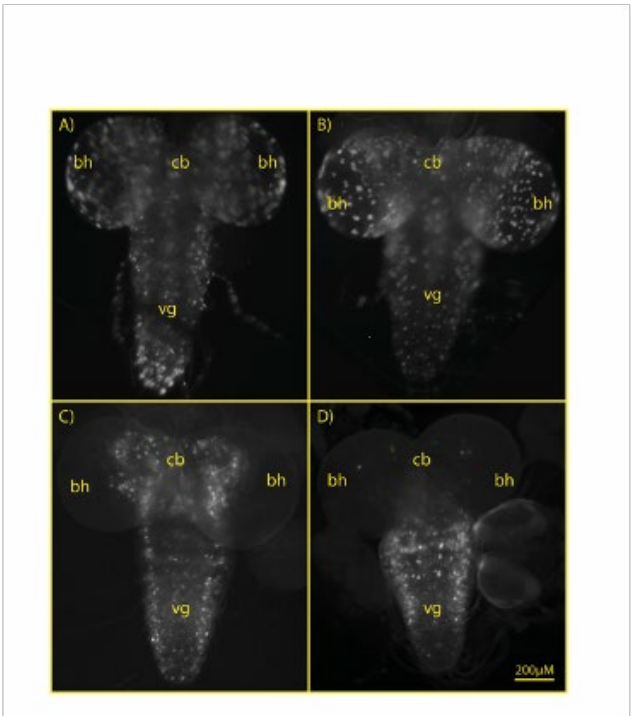

Figure S3 Analysis of *Dα6* enhancer constructs in pStinger vector.
Nuclear green fluorescent protein (nGFP) expressed under control of both the FKBP59_0.6kb enhancer fragment (A-B) and the Dα6_1.1kb enhancer fragment (C-D), demonstrating the different expression patterns from these two DNA fragments. The two different images for each fragment represent the general expression pattern observed in the 3rd instar larval central nervous system and are from individual insertion events to control for possible position effects. All dorsal view. The FKBP59_0.6kb fragment (A-B) shows wide expression throughout the central nervous system, the Dα6_1.1kb (C-D) shows a more restricted expression pattern concentrated in the central brain and ventral ganglion. Images were taken on an Olympus SZX12 stereomicroscope attached to a mercury burner at 400x magnification through a GFP filter. Abbreviations – bh;brain hemisphere, cb; central brain, vg; ventral ganglion. Scale bar = 200µM.

Table S1. MIQE Table

Sample/Template	details	Checklist
Source	If cancer, was biopsy screened for adjacent normal tissue?	Drosophila melanogaster 1st instar
Method of preservation	Liquid N2/RNAlater/formalin	Liquid N2
Storage time (if appropriate)	If using samples >6 months old	< 2 month old
Handling	fresh/frozen/formalin	Frozen
Extraction method	TriZol/columns	TriZol
RNA: DNA-free	Intron-spanning primers/no RT control	Intron-spanning primers, Dnase1, PCR check
Concentration	Nanodrop/ribogreen/microfluidics	Fluorometric Quantitation
RNA: integrity	Microfluidics/5':3' assay	Agarose Gel
Inhibition-free	Method of testing	Dilution curve, PCR efficiency less than 100%
Assay optimisation/validation		
Accession number	RefSeq XX_1234567	NM_001273373.2, NM_001201835.3, NM_205953.3, NM_205952.3, NM_135472.6, NM_205951.2, NM_164874.3
Amplicon details	exon location, amplicon size	243bp
Primer sequence	even if previously published	Dα6L1 CAATATCTGGCTCCCAAACC Dα6R1 TCGTGAAGAGCGTGAAAACAA
Probe sequence*	identify LNA or other substitutions	N/A
In silico	BLAST/Primer-BLAST/in-fold	Primer-BLAST, electrophoresis, melt curve
empirical	primer concentration/annealing temperature	10uM, 61deg
Priming conditions	oligo-dT/random/combination/target-specific	oligo-dT
PCR efficiency	dilution curve	Dα6 =1.79 CG13220=1.86
Linear dynamic range	spanning unknown targets	2 fold serial dilution
Limits of detection	LOD detection/accurate quantification	Dα6 > CT 37, CG13220 > CT 35
Intra-assay variation	copy numbers not Cq	Dα6= 0.19 CG13220=0.16
RT/PCR		
Protocols	detailed description, concentrations, volumes	12.5ul total reaction. 5ul Sybrgreen Master Mix, 0.25ul F, 0.25ul R, 4.5ul H2O and 2.5ul Template
Reagents	supplier, Lot number	QuantiFast SYBR green PCR kit, Qiagen
Duplicate RT	ΔCq	Triplicate
NTC	Cq & melt curves	CT value or melt curve not detected
NAC	ΔCq beginning/end of qPCR	N/A
Positive control	inter-run calibrators	Inter-run Calibrator
Data analysis		
Specialist software	e.g., QBAsePlus	2-ΔΔCT method (Livak and Schmittgen, 2001)
Statistical justification	e.g., biological replicates	3 biological replicates for each cross
Transparent, validated normalisation	e.g., GeNorm summary	Target and housekeeper validated at the same life stage

871
872
873

Table S2. elav>GAL4 x UAS-*α6* corrected mortality (%) results in the *dα6^{nx}* background.

dα6^{nx}	0.05ppm	*95%CI +/-*	0.1ppm	*95%CI +/-*	0.3ppm	*95%CI +/-*
Background Controls						
ΦX-86Fb	**-6%**	*10%*	**-4%**	*9%*	**3%**	*10%*
elav>GAL4	**-11%**	*15%*	**-10%**	*14%*	**-6%**	*16%*
Insertion Parentals						
UAS-Dα6-3b8b	**-6%**	*6%*	**10%**	*5%*	**66%**	*9%*
UAS-Dα6-3a8a	**4%**	*19%*	7%	*18%*	**95%**	*3%*
UAS-Dα6-3b8a	**3%**	*6%*	**8%**	*6%*	**28%**	*6%*
UAS-Dα6-3a8b	**0%**	*14%*	1%	*14%*	**82%**	*5%*
Expression Crosses						
elav>GAL4 x ΦX-86Fb	0%	*9%*	0%	*11%*	2%	*11%*
elav>GAL4 x UAS-Dα6-3b8b	**88%**	*7%*	**99%**	*2%*	**100%**	*0%*
elav>GAL4 x UAS-Dα6-3a8a	**95%**	*4%*	**100%**	*0%*	**100%**	*0%*
elav>GAL4 x UAS-Dα6-3b8a	**75%**	*7%*	**92%**	*3%*	**99%**	*1%*
elav>GAL4 x UAS-Dα6-3a8b	**83%**	*6%*	**99%**	*2%*	**100%**	*0%*

Significant effect on mortality relative to undosed media.

874

875

Table S3. elav>GAL4 x UAS-*α6* corrected mortality (%) results in the *dα6^{W337*}* background

dα6^{W337*}	0.05ppm	*95%CI +/-*	0.1ppm	*95%CI +/-*	0.3ppm	*95%CI +/-*
Background Controls						
ΦX-86Fb	**8%**	24%	**8%**	15%	**5%**	10%
elav>GAL4	**2%**	10%	**0%**	10%	**17%**	24%
Insertion Parentals						
UAS-Dα6-3b8b	**-1%**	10%	**4%**	12%	**66%**	9%
UAS-Dα6-3a8a	**7%**	11%	**26%**	5%	**99%**	1%
UAS-Dα6-3b8a	**5%**	13%	**15%**	15%	**37%**	14%
UAS-Dα6-3a8b	**3%**	15%	**38%**	11%	**99%**	2%
Expression Crosses						
elav>GAL4 x ΦX-86Fb	**-1%**	33%	**-2%**	35%	**0%**	34%
elav>GAL4 x UAS-Dα6-3b8b	**85%**	6%	**99%**	1%	**99%**	1%
elav>GAL4 x UAS-Dα6-3a8a	**77%**	11%	**98%**	3%	**99%**	1%
elav>GAL4 x UAS-Dα6-3b8a	**88%**	4%	**97%**	2%	**95%**	4%
elav>GAL4 x UAS-Dα6-3a8b	**82%**	5%	**99%**	2%	**100%**	1%

Significant effect on mortality relative to undosed media.

Table S4. D*α6>GAL4 x* UAS-Dα6-3b8b corrected mortality (%) results in the *dα6^{W337*}* background

dα6^{W337*}	0.05ppm	*95%CI +/-*	0.1ppm	*95%CI +/-*	0.3ppm	*95%CI +/-*
Parental insertions						
UAS-Dα6-3b8b	**2%**	25%	**11%**	28%	**72%**	8%
Dα6>GAL4	**5%**	13%	**2%**	16%	**-2%**	13%
Expression Cross						
Dα6>GAL4 x UAS-Dα6-3b8b	**32%**	15%	**73%**	7%	**99%**	1%

Significant effect on mortality relative to undosed media.

Table S5. Pest *UAS-α6* expression corrected mortality (%) results in the *dα6^{W337*}* background

dα6^{W337*}	0.05ppm	95%CI +/-	0.1ppm	95%CI +/-	0.3ppm	95%CI +/-	0.5ppm	95%CI +/-	1ppm	95%CI +/-	10ppm	95%CI +/-
Background Controls												
ΦX-86Fb	ND		-1%	17%	2%	13%	4%	18%	13%	13%	77%	11%
elav>GAL4	ND		-1%	14%	-8%	15%	3%	14%	5%	24%	34%	18%
Parental insertions												
UAS-Dα6-3b8b	ND		17%	15%	71%	15%	97%	2%	100%	0%	ND	
UAS-Mdα6-3b8a	ND		ND	8%			1%	7%	23%	9%	99%	1%
UAS-Bovα6-3a8b	ND		ND		ND		2%	7%	7%	10%	ND	
UAS-Pxα6-3a8b	ND		40%	44%	99%	3%	100%	0%	100%	0%	100%	0%
Expression Crosses												
elav>GAL4 x UAS-Dα6-3b8b	73%	5%	94%	4%	100%	1%	100%	0%	100%	0%	100%	0%
elav>GAL4 x UAS-Mdα6-3b8a	ND		19%	17%	66%	9%	93%	4%	99%	1%	ND	
elav>GAL4 x UAS-Bovα6-3a8b	ND		ND		66%	19%	81%	13%	97%	3%	ND	
elav>GAL4 x UAS-Pxα6-3a8b	88%	4%	99%	2%	100%	0%	100%	0%	100%	0%	100%	0%

Significant effect on mortality relative to undosed media.

ND – Not tested at that dose